Theoretical Solar-to-Electrical Energy-Conversion Efficiencies of Perylene−Porphyrin Light-Harvesting Arrays†

Georg M. Hasselman,‡ David F. Watson,‡ Jonathan R. Stromberg,‡ David F. Bocian,*,§ Dewey Holten,*,|| Jonathan S. Lindsey,*,⊥ and Gerald J. Meyer*,‡

Departments of Chemistry and Materials Science and Engineering, Johns Hopkins University, 3400 N. Charles Street, Baltimore, Maryland 21218, Department of Chemistry, University of California Riverside, Riverside, California 92521-0403, Department of Chemistry, Washington University, St. Louis, Missouri 63130-4889, and Department of Chemistry, North Carolina State University, Raleigh, North Carolina 27695-8204

Received: July 18, 2006; In Final Form: September 8, 2006

The efficiencies of organic solar cells that incorporate light-harvesting arrays of organic pigments were calculated under 1 sun of air mass 1.5 solar irradiation. In one set of calculations, photocurrent efficiencies were evaluated for porphyrin, phthalocyanine, chlorin, bacteriochlorin, and porphyrin−bis(perylene) pigment arrays of different length and packing densities under the assumption that each solar photon absorbed quantitatively yielded one electron in the external circuit. In another more realistic set of calculations, solar conversion efficiencies were evaluated for arrays comprising porphyrins or porphyrin−$(perylene)_2$ units taking into account competitive excited-state relaxation pathways. A system of coupled differential equations for all reactions in the arrays was solved on the basis of previously published rate constants for (1) energy transfer between the perylene and porphyrin pigments, (2) excited-state relaxation of the perylene and porphyrin pigments, and (3) excited-state electron injection into the semiconductor. This formal analysis enables determination of the optimal number of pigments in an array for solar-to-electrical energy conversion. The optimal number of pigments depends on the molar absorption coefficient and the density at which the arrays can be packed on an electrode surface. Taken together, the ability to employ fundamental photophysical, kinetic, and structural parameters of modular molecular architectures in assessments of the efficiency of solar-to-electrical energy conversion should facilitate the design of molecular-based solar cells.

Introduction

The inspiration of photosynthesis has prompted considerable interest in utilizing organic pigments for solar-energy applications. The theoretical conversion efficiency of photosynthetic systems has been widely discussed and is closely related to the question of why plants are green.[1] Shockley and Queisser calculated the maximum solar-to-*electrical* energy conversion efficiency from a single junction photovoltaic cell to be about 31% (1 sun, air mass (AM) 1.5 spectral distribution).[2] This celebrated limit was calculated under the assumption that the energy of solar photons that exceeds the semiconductor band gap, E_g, cannot be utilized (due to thermalization losses that result in equilibration to E_g). Ross and Nozik later showed that the theoretical efficiency can exceed 60% if the electron and hole from the photogenerated electron−hole pair can be collected in the external electrical circuit prior to thermalization to the semiconductor's conduction and valence band edge levels, respectively.[3] These same optimal efficiencies apply to organic solar cells. The maximum photocurrent can be calculated from the overlap of the pigment's absorptance spectrum with the solar spectrum. Within the Shockley−Queisser limit, the upper limit of the power-conversion efficiency involves the product of this photocurrent and the free energy stored in the thermally equilibrated excited state.

A major challenge in designing molecular-based solar cells lies in the choice and organization of the light-absorbing pigments. Efficient solar energy conversion requires light absorption over a broad spectral range in the visible and near-infrared regions. Photosynthetic pigments related to the chlorophylls are particularly promising light absorbers for solar cell applications, owing to their large molar absorption coefficients, tunable photophysical properties, and amenability to molecular modification. The harvesting of sunlight on a planar surface requires multiple layers of pigments, given that a monolayer of pigments absorbs only a small fraction of the incident light. A key issue that has not been addressed, to our knowledge, concerns how the multilayer thickness of given types of organic pigments affects the efficiency of light harvesting. Understanding the interplay of multilayer thickness and light-harvesting efficiency is essential for the systematic design of solar cells that incorporate molecular-based antennas.

Recent synthetic advances have allowed the preparation of linear, semirigid light-harvesting arrays that consist of porphyrin pigments linked together by diphenylethyne groups.[4−6] The electrochemical and visible-region absorption properties of these arrays, which reflect properties of the ground and lowest excited singlet states, are accurately modeled as a sum of the properties

† Part of the special issue "Arthur J. Nozik Festschrift".

* Email addresses: meyer@jhu.edu (G.J.M.); David.Bocian@ucr.edu (D.F.B.); holten@wustl.edu (D.H.); jlindsey@ncsu.edu (J.S.L.).
‡ Johns Hopkins University.
§ University of California Riverside.
|| Washington University.
⊥ North Carolina State University.

10.1021/jp064547x CCC: $33.50
Published on Web 11/23/2006

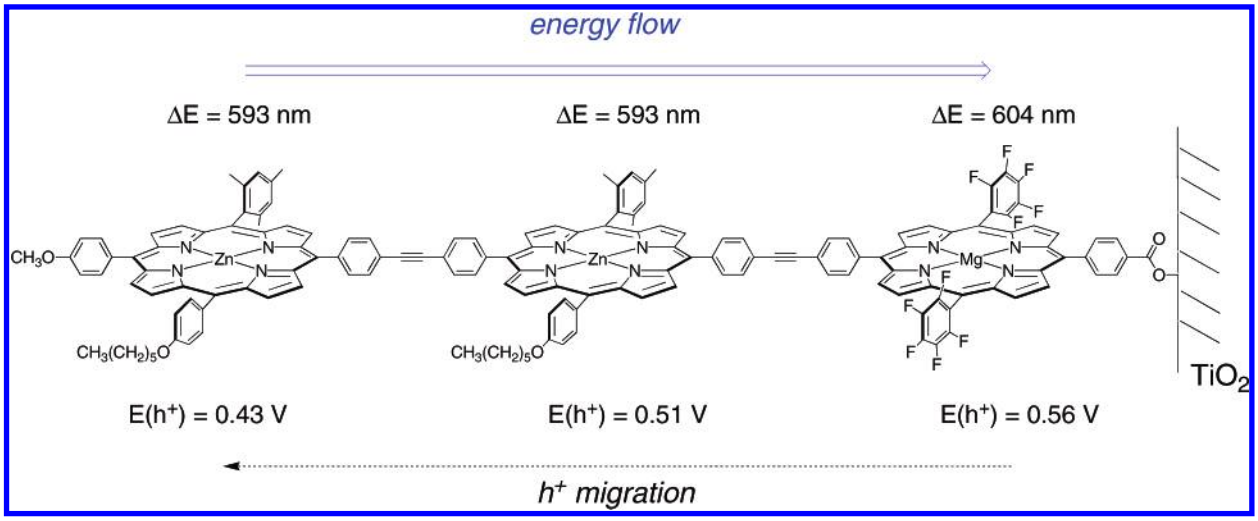

Figure 1. A porphyrin triad that promotes energy and hole transfer in opposite directions.

of the individual porphyrin subunits.[7] Electronic coupling through the diphenylethyne linkages is weak yet suffices to allow rapid intramolecular excited-state energy transfer and ground-state electron/hole transfer.[7] Singlet excited-state energy transfer occurs on the picosecond time scale, predominantly via a through-bond mechanism. Intramolecular hole transfer in the one-electron oxidized form of the arrays occurs on a submicrosecond time scale.[7−9] These rapid energy-transfer and electron/hole-transfer processes afford nearly quantitative excited-state energy migration and ground-state hole migration over long distances through multiporphyrin arrays.[4,6,7]

The attractive photophysical properties of multiporphyrinic arrays make such arrays intriguing candidates for use in solar cells. In the simplest case, one end of a linear array could be attached to the surface of a semiconductor through an appropriate binding group. For example, an array consisting of three different porphyrin pigments is shown in Figure 1.[10] Light absorption by a remote pigment is followed by singlet−singlet excited-state energy transfer along the array, terminating at the porphyrin pigment directly anchored to the semiconductor surface. This terminal porphyrin serves as the electron injection unit. The redox potentials of the porphyrins in the array shown in Figure 1 were designed such that the oxidized equivalent (hole) would move away from the semiconductor toward the counter electrode, where the hole could be intercepted by a hole-transport material.

The fraction of solar photons absorbed by porphyrins is quite small, because the dominant absorption band of porphyrins lies in the near-UV region. Light harvesting in principle can be improved by utilizing structurally related chromophores that absorb strongly in the red or near-infrared region, such as chlorins, bacteriochlorins, and phthalocyanines (Chart 1), though the synthetic methods for manipulating such compounds in arrays are comparatively undeveloped at present. Alternatively, accessory pigments with complementary absorption properties can be covalently bound to the macrocyclic pigments. Toward this end, perylene−imide dyes covalently attached to porphyrins have been synthesized that increase light harvesting in the blue-green region, i.e., between the porphyrin Soret and Q-bands.[4,5,11−26] Excitation of the perylene is followed by nearly quantitative energy transfer to the porphyrin, promoting the porphyrin to its singlet excited state. Subsequent energy-transfer processes along an array comprising these pigments occurs efficiently. One example of a linear array composed of porphyrin−(perylene)$_2$ units is shown in Chart 2.[5,23] Other porphyrin−(perylene)$_n$ monomers (n = 1, 2, and 4) in different architectures

CHART 1: Types of Pigments Examined Herein

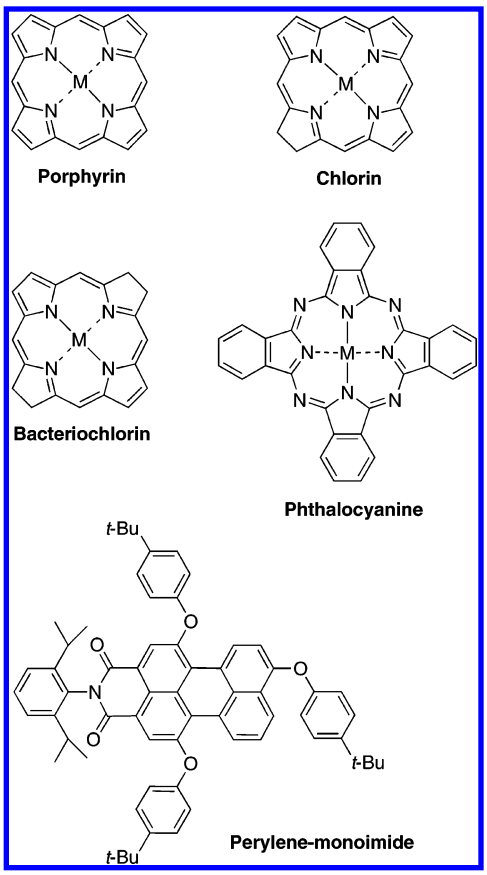

(and a range of expected footprint sizes) have been prepared and converted to the corresponding diphenylethyne- or diphenylbutadiyne-linked oligomeric arrays.[5]

The goal of the present study is to theoretically predict the efficiency of a regenerative solar cell containing arrays of porphyrinic pigments anchored to a planar, transparent semiconductor surface. This architecture of multiporphyrin arrays on a planar semiconductor is quite different from the dye-sensitized high-surface-area nanocrystalline thin films pioneered by Gratzel (which also have been extensively modeled[27]). Indeed, the use of arrays on a single-crystal semiconductor more closely resembles the sensitization studies described by Gerischer, Spitler, Sutin, and others decades ago.[28−30] Because the density of surface states is expected to be lower in a single crystal than

CHART 2: A Diphenylethyne-Linked Array (Oligo-18 in ref 5) Wherein the Monomer Unit Contains One Porphyrin and Two Perylene Accessory Pigments, Denoted Porphyrin−(perylene)$_2$

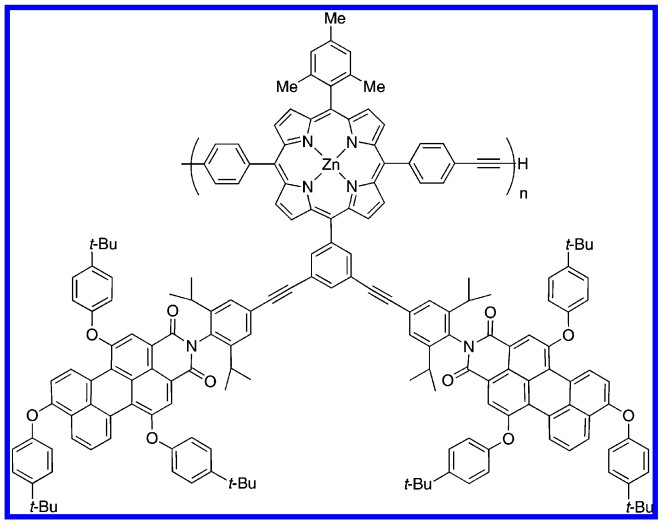

in a mesoscopic nanocrystalline thin film, improved charge transport and increased open-circuit photovoltages may result. While the proposed solar cells utilize arrays of the type shown in Figure 1, such cells could also be constructed from other types of molecules that are weakly coupled electronically (i.e., where key spectral properties of the pigments are relatively unchanged upon incorporation into antennas) including noncovalently linked assemblies. This approach may be modified to incorporate changes in spectral characteristics upon increasing the number of chromophores in the assembly due to interchromophore and other interactions.

The organization of this manuscript is as follows. We first focus on the fraction of sunlight harvested by arrays comprising the pigments of the type shown in Charts 1 and 2 under AM 1.5 solar standard conditions. We initially assume that all of the absorbed light is converted to electricity, which gives the maximum theoretical photocurrent that the pigments in Charts 1 and 2 could produce under AM 1.5 solar irradiation. We then calculate more realistic photocurrent efficiencies by taking into account the nonunity electron-collection efficiency of absorbed photons. These calculations utilize energy migration and excited-state relaxation rate constants that have been previously measured for small arrays in fluid solution. On the basis of the modeled properties of the porphyrin and porphyrin−perylene arrays, we propose additional (as yet unprepared) arrays that should have higher photocurrent efficiencies. We emphasize again that the approach described herein is general and could be applied to arrays containing other organic dyes, transition metal compounds, or quantum dots.

Experimental Methods

Light Harvesting and Photocurrent Efficiencies of Surface-Anchored Arrays. Porphyrins have an intense B (Soret) band near 420 nm with a molar absorption coefficient, ϵ, of roughly 400 000 M^{-1} cm^{-1}, and weaker Q-bands at lower energy. Both of these absorption contours are due to $\pi \rightarrow \pi^*$ transitions that are polarized in the plane of the porphyrin ring. For porphyrins that have approximate D_{4h} symmetry (such as those shown in Chart 1), both the B and Q excited states are doubly degenerate (planar oscillators). Consequently, the measured molar absorption coefficient for each transition is the sum of the two degenerate components of the planar oscillator. If the porphyrin arrays are aligned perpendicular to the electrode surface and the light impinges along the surface normal, the transition dipole moment of one of the two transitions of the planar oscillator will be orthogonal to the electric-field vector of the incident radiation; thus, the effective molar absorption coefficient of the porphyrin B or Q transitions for the surface-attached species will be half of that measured in solution.[31] This effective molar absorption coefficient will increase if the porphyrin or porphyrin-based array is tilted on the surface or if light impinges at an angle with respect to the surface normal. Regardless, for the purposes of this study, we assume that the molar absorption coefficient of each porphyrin transition is halved from the solution value. Similarly, we assume a 50% decrease in the effective molar absorption coefficient for a perylene−monoimide pigment in the surface-adsorbed arrays. The perylene pigments have molar absorption coefficients of roughly 32 000 M^{-1} cm^{-1} in fluid solution.[23] The perylenes may adopt a variety of orientations within the array; thus, the 50% decrease represents a worst-case scenario.

In keeping with previous findings, the visible Q-region absorption contour of an array of porphyrinic pigments covalently linked via diphenylethyne bridges is well-modeled as the sum of the spectra of the individual pigments, consistent with weak electronic coupling between the pigments in the array.[7] This is not the case for the Soret-region spectral contour, for which dipole−dipole exciton coupling or aggregation effects cause the band shape to deviate from that of a porphyrin monomer. These electronic effects will clearly have an influence on the properties of the porphyrin-based solar cells but are not considered in the present analysis to simplify the spectral modeling.

The efficiency of a solar cell is related to the absorptance, α, which is sometimes called the "light-harvesting efficiency" in the photoelectrochemical literature. The absorptance is the fraction of light absorbed or, equivalently, the probability for photon absorption. In the absence of light scattering, the absorptance is equal to 1 minus the transmittance and can be related to the molar absorption coefficient, ϵ, through the optical cross section (σ), where σ (Å^2) = $(3.82 \times 10^{-5}) \times \epsilon$.[32] The absorptance is then the ratio of the optical cross section to the area occupied on a planar surface, i.e., the "footprint". If all of the incident light reaches the absorber, then we denote the absorptance as α_1, which is given by

$$\alpha_1 = \sigma\,(\text{Å}^2)/\text{footprint}\,(\text{Å}^2) = 3.82 \times 10^{-5} \cdot \epsilon/\text{footprint} \quad (1)$$

Sunlight will nominally enter the array-containing solar cells through the transparent semiconductor material and is therefore most strongly absorbed by the pigment directly attached to the surface. Light transmittance decays exponentially through the array. The probability of photon absorption by the *n*th pigment in the array is given by eq 2

$$p_n = (1 - \alpha_1)^{n-1} \cdot \alpha_1 = 10^{(-\beta \cdot n)} \quad (2)$$

where $\beta = -\log(\alpha_1)$. In other words, the fraction of the total irradiance absorbed by the *n*th pigment in an array (p_n in eq 2) is attenuated due to light absorption by pigments closer to the surface (and the light source). Summation of the probability of the total irradiance absorbed by each

pigment along the length of the array gives the fraction of light absorbed by the entire array, namely, the total absorptance

$$\alpha = \sum_{1}^{n} p_n \tag{3}$$

Two additional parameters that characterize a solar cell include (1) the *incident* photon-to-current efficiency (IPCE), defined as the (number of injected electrons in the external circuit)/(number of photons incident on the solar cell), and (2) the *absorbed* photon-to-current efficiency (APCE), defined as the (number of injected electrons in the external circuit)/(number of photons absorbed by the solar cell). The α, IPCE, and APCE values are unitless and can vary from zero to unity as a function of the wavelength of light. The total absorptance, α, places an upper limit on the photocurrent efficiency. For an idealized solar cell, the IPCE is equal to α, and the APCE is unity. We note that an APCE of unity is often reported for Gratzel-type solar cells.

The total photocurrent of an idealized solar cell under AM 1.5 solar irradiation conditions, i_{sc}, can be calculated with knowledge of the number of photons available at each frequency. To do so, the AM 1.5 solar spectrum (available from the NREL website at www.nrel.gov) must be converted from power/wavelength to photons/frequency. Then, the photocurrent at each frequency can be calculated from the absorptance of the pigments. Integration over all frequencies of light gives i_{sc}. Note that i_{sc} has units of current (amperes) and is often expressed as a current density, A/cm^2, to account for the electrode size. The method of calculating i_{sc} when the APCE is not unity is described further below.

The spectral properties of the porphyrins (and related pigments) that are required to determine the absorptance (α) are available in a published database.[33] A lower limit of the footprint of the porphyrin array would be the product of the in-plane and out-of-plane van der Waals radii of the porphyrinic pigment (again assuming that the array is normal to the surface). However, many factors will control the actual size of the footprint of an array, including interarray interactions, the density of surface binding sites, and the size of the surface-anchoring group.[34] Therefore, we consider a variety of footprints that span a range from unrealistically small to unrealistically large for the porphyrinic arrays, but which may be generally useful for determining the light-harvesting and solar-energy-conversion efficiencies of other classes of pigments.

Theoretical Maximum Global Efficiencies. Global efficiencies (η) were calculated according to eq 4, where I_o is the irradiance of the AM 1.5 illumination, which is ∼100 mW/cm^2, i_{sc} is the total photocurrent (or current density) described above, and the fill factor (ff) is equal to 1.

$$\eta = \frac{i_{sc} V_{oc} \mathrm{ff}}{I_o} \tag{4}$$

In eq 4, V_{oc}, the open-circuit voltage, represents the maximum Gibbs free energy that can be abstracted from a regenerative solar cell. The value of V_{oc} was approximated as $E_{00} - 2{\cdot}\lambda_{inj}$, where E_{00} is the relevant excited-state energy of the sensitizer, and λ_{inj} is the reorganization energy for excited-state electron injection. This estimate for V_{OC} is used, because in the Gerischer model, the maximum electron-injection efficiency is obtained when the excited-state reduction potential is above (closer to the vacuum level) the conduction band energy by twice λ_{inj}.[28] For a given porphyrin-containing array, E_{00} for the porphyrin closest to the semiconductor was approximated from the average of the $Q(0, 0)$ absorption and fluorescence energies; the value of λ_{inj} is assumed to be 0.35 V, consistent with experimentally determined values for interfacial electron injection.[28−30,34] Thus, for a zinc porphyrin, this calculation gives $V_{oc} \approx (2.08 - 2{\cdot}0.35)$ V = 1.4 V. We emphasize that V_{oc} values greater than 1.4 V and fill factors of unity are without precedence in the organic photovoltaic literature, and these values represent optimal efficiencies. The theoretical efficiency with other values of V_{oc} and ff are easily calculated. Some examples are described further below.

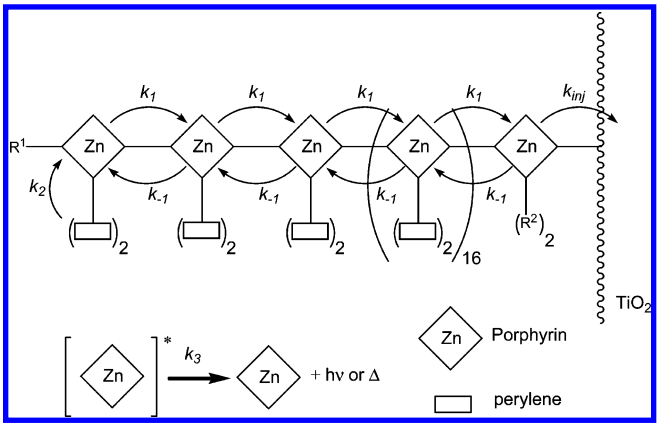

Figure 2. Rate constants for excited-state energy transfer (k_1 and k_{-1}), electron injection (k_{inj}), and excited-state deactivation in the absence of energy transfer or electron transfer (k_3) within an array consisting of 20 porphyrin pigments and 38 perylene pigments attached to a TiO_2 semiconductor surface. R^1 and R^2 correspond to non-chromophoric substituents at the meso positions of the porphyrins.

Kinetic Modeling. A more realistic approach for predicting photocurrent efficiency would incorporate the fact that photon absorption within a light-harvesting array will not lead to a unity yield of electron injection into the semiconductor. This will lead to IPCE values smaller than those calculated from the absorptance (including light attenuation along the array given by eq 2) and, similarly, APCE values less than unity. This is so because the desired energy transfer at each step is in competition with the intrinsic excited-state deactivation processes of the corresponding pigment within the array. The effects of these competitive processes on the overall yield for electron injection can be garnered through kinetic modeling, which involves solution of the associated set of coupled differential equations. The methods described by van Patten et al.[35] allow one to compute the efficiency of excited-state energy migration through an array under conditions where the individual rate constants are known.

Figure 2 depicts a model for an array that consists of 20 zinc porphyrin and 38 perylene units wherein the 2 perylenes are attached on the same side of the porphyrin via 1 meso substituent (as shown in Chart 2). Each porphyrin except the one closest to the semiconductor is substituted with perylene accessory pigments. Because perylene-to-porphyrin energy transfer is substantially downhill energetically (effectively irreversible), it is mathematically equivalent to treat the 2 perylenes on each porphyrin as 1 perylene with a molar absorption coefficient twice as large. The rate constants for energy transfer from perylene to porphyrin (k_2) and between porphyrins (k_1 and k_{-1}) are known from model systems and are assumed not to change significantly as the size of the array increases.[4−7] If the excitation reaches the terminal porphyrin, an electron can be injected into the semiconductor with rate constant k_{inj}. The combined rate constant for excited-state deactivation (by radiative and non-

TABLE 1: Total Absorptance of Porphyrin Arrays at the Soret-band Maximum with the Indicated Number of Pigments (n) and Footprint Sizes[a]

footprint [Å^2]	absorptance				
	$n = 1$	$n = 5$	$n = 10$	$n = 20$	$n = 50$
25	0.306	0.839	0.974	0.999	1.000
50	0.153	0.564	0.810	0.964	1.000
100	0.0764	0.328	0.549	0.796	0.981
115	0.0665	0.291	0.498	0.748	0.968
150	0.0510	0.230	0.408	0.649	0.927
225	0.0340	0.159	0.292	0.499	0.823
300	0.0255	0.121	0.228	0.403	0.725
400	0.0191	0.0920	0.176	0.320	0.619
500	0.0153	0.0742	0.143	0.265	0.537
625	0.0122	0.0597	0.116	0.218	0.460

[a] An optical cross section $\sigma = 7.64$ Å^2, corresponding to a molar absorption coefficient $\epsilon = 200\,000$ M^{-1} cm^{-1}, at the Soret-band maximum (~420 nm), was used for the calculation. The calculations utilized eqs 1−3.

radiative processes) in the absence of energy transfer or electron transfer is k_3 for a zinc porphyrin and k_4 for a perylene (not shown in Figure 2).

The above kinetic processes (rate constants k_1 to k_4 and k_{-1}) form the backbone of the kinetic model depicted in Figure 2. The corresponding system of coupled differential equations can be solved, and values for the rate constants derived from previous studies can be utilized, as described in the Appendix. The initial condition for a given kinetic simulation is the fraction of the excitation that initially resides on each pigment. We term this starting condition the "initial absorptance profile". For some cases, this profile is derived from absorptance-per-pigment calculations that takes into account the fact that light transmittance falls off exponentially across the array with increasing distance from the transparent semiconductor surface (see eq 2). In some cases an excitation was placed on a given pigment. Kinetic modeling is then used to compute how efficiently the initial excitation having a given site distribution ultimately leads to injection of an electron into the semiconductor. We assume for the purpose of this paper that the hole left behind in the form of an oxidized porphyrin is reduced by an external donor with unity yield. The calculation of the IPCE was performed at each wavelength.

Results and Discussion

Light-Harvesting Efficiencies of Surface-Adsorbed Arrays. The total absorptance (α, calculated via eqs 1−3) of porphyrin arrays at the Soret maximum (~420 nm) is given in Table 1 as a function of the number of pigments in the array and the size of the footprint on a planar surface. Note that a 50-porphyrin array with an idealized footprint of 115 Å^2 absorbs >97% of the incident light. Increasing the number of porphyrins in the array above 50 will not have a significant influence on the light-harvesting efficiency in the Soret region but would improve harvesting at longer wavelengths where the molar absorption coefficient is lower (i.e., in the Q-band region).

Table 1 reveals that the fraction of light absorbed by an array of pigments organized on a planar surface depends strongly on the footprint of the array. This raises the question of how tightly one could expect to assemble such arrays. The minimum footprint would be ~115 Å^2 for a porphyrin macrocycle of van der Waals dimensions (5 × 20 Å^2) with an appended phosphonate group binding to the 100 face of anatase TiO_2 (Figure 3). A porphyrin bearing two perylene units (Chart 2) would be expected to have a footprint of roughly 300−500 Å^2. For consistency across a number of the calculations described below, we have arbitrarily chosen a value of 115 Å^2.

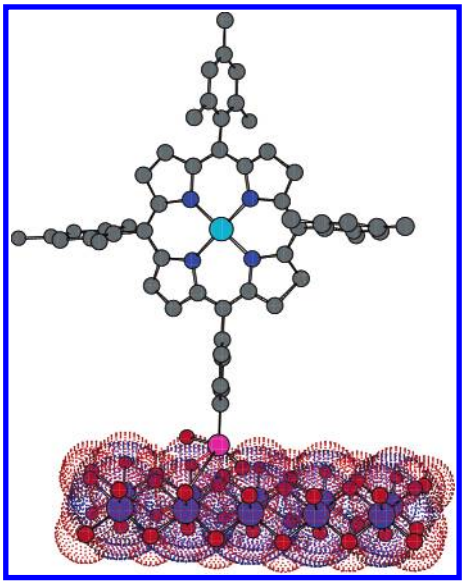

Figure 3. Geometry of a porphyrin anchored to a metal oxide semiconductor surface through a phosphoester linkage. Linear arrays would extend outward, perpendicular to the surface with diphenylethyne linkages between adjacent macrocycles. gray dot = carbon, blue dot = nitrogen, cyan dot = porphyrin metal ion, magenta dot = phosphorus, red dot = oxygen.

Figure 4A shows the absorptance spectra of surface-bound arrays comprising different numbers of porphyrin−(perylene)$_2$ units (see Chart 2 for unit structure), assuming a footprint of 115 Å^2 on a planar surface. These spectra were calculated by scaling (multiplying) the absorption (A) spectrum of an array consisting of a single porphyrin−(perylene)$_2$ unit by the desired number of units in the oligomeric array (1 to 50) and then converting to absorptance (α) using the relationship $\alpha = 1-10^{-A}$. Figure 4B shows the total Soret band absorptance as a function of the number of porphyrin−(perylene)$_2$ units. For $\sigma = 7.64$ Å^2 ($\epsilon = 200\,000$ M^{-1} cm^{-1}), the fraction of light in the Soret region absorbed by each porphyrin is 0.0664 and the light transmitted is attenuated to (1 − 0.0664) = 0.9336 of the incident irradiance. A monolayer of linear arrays with 20 porphyrins per array, aligned perpendicular to the surface and parallel to the incoming light, absorbs 0.747 (~75%) of the light with 0.018 (~2%) contributed by the 20th (distal) porphyrin.

Theoretical Maximum Global Efficiencies. Table 2 shows the dependence of the theoretical maximum global efficiency (η) on the footprint of the arrays comprising porphyrin−(perylene)$_2$ units. As expected, the theoretical maximum global efficiency varies greatly with the number of pigment units and the footprint on the electrode. Table 3 shows theoretical maximum global efficiencies for representative porphyrin, porphyrin−(perylene)$_2$, phthalocyanine, chlorin, and bacteriochlorin arrays, each with a footprint of 115 Å^2. Inspection of the predicted efficiencies reveals the importance of maximizing the overlap of the array absorptance and the solar spectrum. For example, the predicted global efficiency for phthalocyanine arrays of a given length is more than twice the efficiency of porphyrin arrays of the same length. This occurs because the Q-band absorption of a phthalocyanine is significantly larger and to the red of that of a porphyrin. Indeed, the phthalocyanine Q-band is centered at ~650 nm, near the most intense region of the AM 1.5 solar spectrum (see Figure 4). (The phthalocyanine Soret band at ~350 nm makes markedly less of a contribution due to poor overlap with the solar spectrum.) In

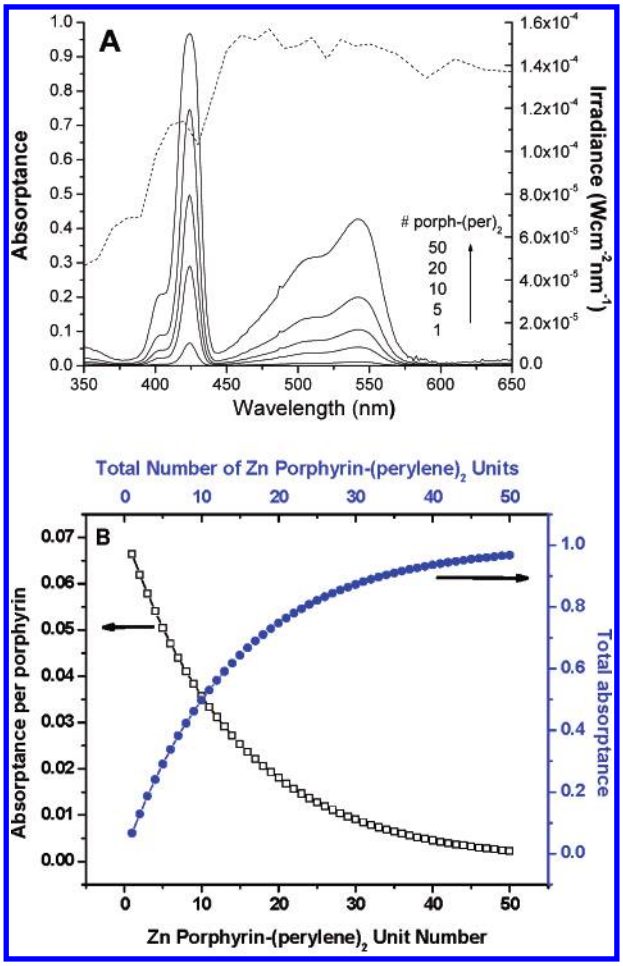

Figure 4. (A) Absorptance spectra of arrays comprising different numbers of porphyrin−(perylene)$_2$ units, assuming a footprint of 115 Å^2 on a planar electrode. Superimposed on the (calculated) spectral data is the AM 1.5 solar irradiance spectrum (- - -). (B) Soret band absorptance of each porphyrin−(perylene)$_2$ pigment in a 50-mer array (squares) and the total absorptance of arrays with the indicated number of porphyrin−(perylene)$_2$ units (circles). Note that the unit closest to the array (unit 1) does not have perylenes attached to the zinc porphyrin, as indicated in Figure 2.

TABLE 2: Theoretical Maximum Global Efficiencies (η), Expressed as a Percentage, for Arrays of Porphyrin−(Perylene)$_2$ Units under AM 1.5 Solar Illumination as a Function of Array Footprint and the Number of Pigment Units, n[a]

footprint [Å^2]	theoretical maximum global efficiency (%)				
	$n = 1$	$n = 5$	$n = 10$	$n = 20$	$n = 50$
25	0.54	2.27	3.88	6.24	10.32
50	0.25	1.11	1.99	3.37	6.10
100	0.14	0.65	1.22	2.23	4.51
115	0.12	0.57	1.08	1.97	4.06
150	0.08	0.40	0.76	1.40	2.94
225	0.05	0.27	0.52	0.98	2.14
300	0.04	0.20	0.39	0.76	1.69
400	0.03	0.15	0.30	0.58	1.32
500	0.02	0.12	0.24	0.47	1.09
625	0.02	0.11	0.21	0.42	0.99

[a] $V_{oc} = 1.4$ V; ff = 1.

contrast, the porphyrin spectrum is dominated by the strong Soret band at ∼420 nm, which occurs in a less intense region of the solar spectrum compared to the phthalocyanine Q-bands. Thus, the redistribution of intensity from the Soret to the Q-band in phthalocyanines versus porphyrins affords greater absorption

TABLE 3: Theoretical Maximum Global Efficiencies (η) for Porphyrinic Arrays (footprint 115 Å^2) with $n = 1$, 5, 10, 20, and 50 Pigments (or multipigment units) under AM 1.5 Solar Illumination

pigment	σ (Å^2)	n	V_{oc} (V)	i_{sc} (A/cm^2)	η (%)
porphyrin[a]	7.64 (Soret)	1	1.4	4.05×10^{-5}	0.06
	0.34 (Q)	5		1.89×10^{-4}	0.26
		10		3.48×10^{-4}	0.49
		20		6.05×10^{-4}	0.85
		50		1.12×10^{-3}	1.57
porphyrin−(perylene)$_2$[b]	7.64 (Soret)	1	1.4	8.43×10^{-5}	0.12
	1.22 (perylene)	5		4.04×10^{-4}	0.57
		10		7.69×10^{-4}	1.08
		20		1.41×10^{-3}	1.97
		50		2.90×10^{-3}	4.06
phthalocyanine[c]	3.06 (Q)	1	1.1	9.80×10^{-5}	0.11
		5		4.78×10^{-4}	0.53
		10		9.27×10^{-4}	1.03
		20		1.75×10^{-3}	1.94
		50		3.73×10^{-3}	4.14
chlorin[d]	1.91 (Soret)	1	1.2	1.81×10^{-5}	0.02
	0.33 (Q)	5		8.92×10^{-5}	0.11
		10		1.75×10^{-4}	0.21
		20		3.38×10^{-4}	0.41
		50		7.69×10^{-4}	0.93
bacteriochlorin[e]	1.91 (Soret)	1	1.2	5.42×10^{-5}	0.07
	0.92 (Q)	5		2.68×10^{-4}	0.32
		10		5.30×10^{-4}	0.64
		20		1.04×10^{-3}	1.26
		50		2.04×10^{-3}	2.46

[a] Zn(II)-5-(3,5-diethynylphenyl)-10,15,20-trimesitylporphyrin (compound **6** in ref 23). [b] Zinc(II)-5-[3,5-bis[2-[4-[1,6,9-tris(4-*tert*-butylphenoxy)perylene-3,4-dicarboximido]-3,5-diisopropylphenyl]ethynyl]phenyl]-10,15,20-trimesitylporphyrin (a benchmark for the monomer composed of two perylene monoimides and one zinc porphyrin; compound **14** in ref 23). [c] Phthalocyanine (the free base species).[35−37] [d] Zn(II)-5-(3,5-di-*tert*-butylphenyl)-10-(4-ethynylphenyl)-17,18-dihydro-18,18-dimethyl-17-oxoporphyrin (an oxochlorin; compound **Oxo-Zn4** in ref 38). [e] Bacteriochlorophyll *a*.[35,39]

of solar energy for phthalocyanines, despite the fact that phthalocyanines exhibit about one-half the total oscillator strength across the visible region versus that of porphyrins. Similarly, chlorins and bacteriochlorins, which absorb strongly in the red region, afford higher efficiencies than porphyrins. The most favorable situation would be to utilize a combination of these chromophores (and other accessory pigments) to utilize their complementary spectral properties to capture the breadth of the solar spectrum.

Table 3 also gives the maximum photocurrent densities that can be achieved from monolayers on a planar surface under AM 1.5 solar irradiation. It is not possible for a monolayer of porphyrins to yield more than ∼40 μA/cm^2 or for a phthalocyanine to yield ∼100 μA/cm^2. We emphasize that the photocurrent densities are calculated directly from the overlap of the pigment's absorptance spectrum with the AM 1.5 solar standard spectrum. The power conversion efficiency determination, on the other hand, requires some assumptions about the fill factor and open-circuit photovoltages.

Kinetic Modeling. Kinetic modeling was performed to account for the multiple relaxation pathways available following light absorption by a single pigment in the array, thereby enabling more accurate prediction of the overall electron-injection yield (i.e., APCE < 1) and hence the solar-conversion efficiency. We first compute the probability that an electron is injected into the semiconductor if an individual porphyrin in a porphyrin−(perylene)$_2$ array absorbs a photon (Figure 5).

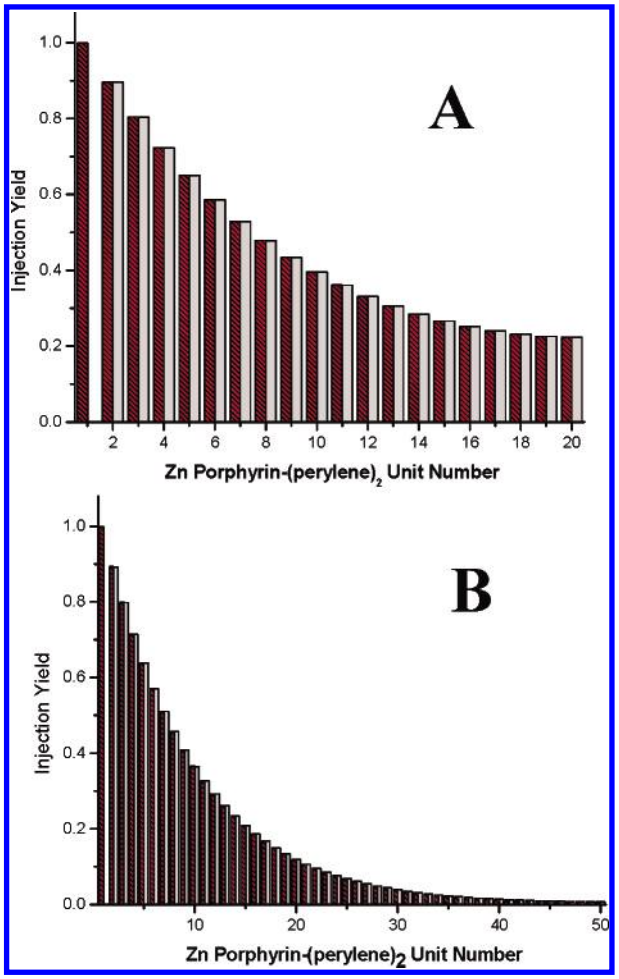

Figure 5. Electron injection yield upon excitation of a given pigment in an array containing porphyrin−(perylene)$_2$ units for (A) 20-mer and (B) 50-mer where porphyrins = dark bars and perylenes = light bars. Note that the unit closest to the array (unit 1) does not have perylenes attached to the zinc porphyrin, as indicated in Figure 2.

In our analysis, we assume that electron injection occurs only when the excited-state energy has migrated to the porphyrin attached to the semiconductor surface. This assumption is inherently reasonable, because injection from pigments distal to the surface would necessarily have to occur via a through-space electron-transfer process over a large distance. The calculations assume that the semiconductor works effectively as a kinetic trap for the excited-state energy. This assumption is also reasonable because excited-state electron injection into wide band gap semiconductors such as TiO_2 is known to occur on a picosecond-to-femtosecond time scale for organic and inorganic pigments.[40] This rate is much faster than the rate of energy transfer along the array or the rates of radiative and nonradiative processes. These latter processes do, however, influence the overall efficiency of electron injection, as is described below.

Our analysis predicts that, in an icosamer (20 porphyrin−(perylene)$_2$ subunits), excitation of the 20th unit leads to injection with a probability of 0.223, but in a 50-mer (50 porphyrin−(perylene)$_2$ subunits), the probability drops to 0.119 for the 20th unit. The drop in efficiency with increased array length is due to the fact that energy migration along an array occurs in both directions with equal probability. The injection yields increase when ZnP*−ZnP → ZnP−ZnP* energy transfer along the array is faster. For example, when this rate constant for energy transfer along the array backbone was increased from $(30\ ps)^{-1}$ to $(5\ ps)^{-1}$, excitation of the 20th unit leads to injection

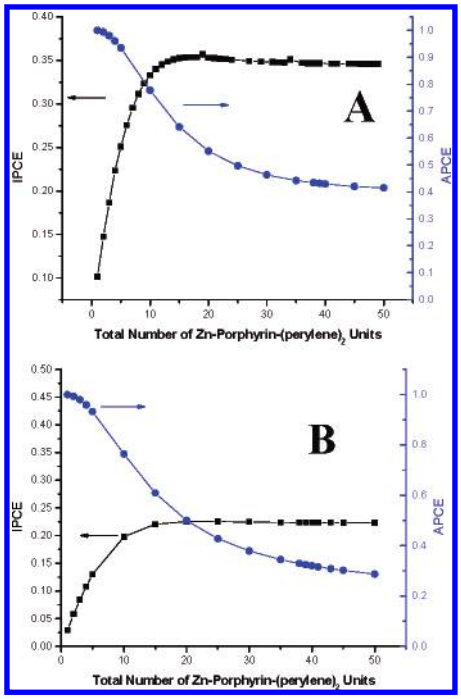

Figure 6. The incident photon-to-current efficiency (IPCE) and the absorbed photon-to-current efficiency (APCE) at the Soret absorption band maximum as a function of the number of porphyrin−(perylene)$_2$ units for two different footprints, (A) 115 Å^2 and (B) 260 Å^2.

with a probability of 0.702 and 0.441 for the 20-mer and 50-mer, respectively. While the longer arrays absorb more light, they also allow for greater losses through radiative or nonradiative decay. Accordingly, there is a penalty for increasing the length of an array beyond a certain point, because excited-state decay pathways play an increasingly important role in reducing the overall efficiency. The efficiency of electron injection resulting from excitation of a perylene is slightly (a few percent) lower than that obtained upon excitation of the porphyrin in the same porphyrin−(perylene)$_2$ unit because of the additional decay pathway

$$\text{perylene}^* \xrightarrow{k_4} \text{perylene} + h\nu \text{ or } \Delta$$

The calculations of light absorption and energy transfer shown above can now be combined in a straightforward way. The initial absorptance profile (Figure 4B) shows the average contribution to light absorption by each porphyrin or perylene pigment. The absorptance data were multiplied by the injection yield to obtain the incident-photon-to-current efficiency (IPCE) for each pigment in the array. Dividing by the fraction of incident photons that were absorbed yields the absorbed photon-to-current efficiency (APCE).

The results of two calculations are shown wherein the footprints were 115 Å^2 (Figure 6A) and 260 Å^2 (Figure 6B). Intuitively, one might assume that, by packing the arrays closer to each other on the surface, the IPCE would just be scaled. However, it turns out that the optimal length is shorter for the more closely packed arrays (Figure 6A). This can be attributed to the fact that photons absorbed closer to the electrode surface more efficiently give rise to electron injection than those absorbed further away. Longer arrays again allow for more losses through excited-state decay. Similar calculations can be made for the perylene units. Because the perylene molar

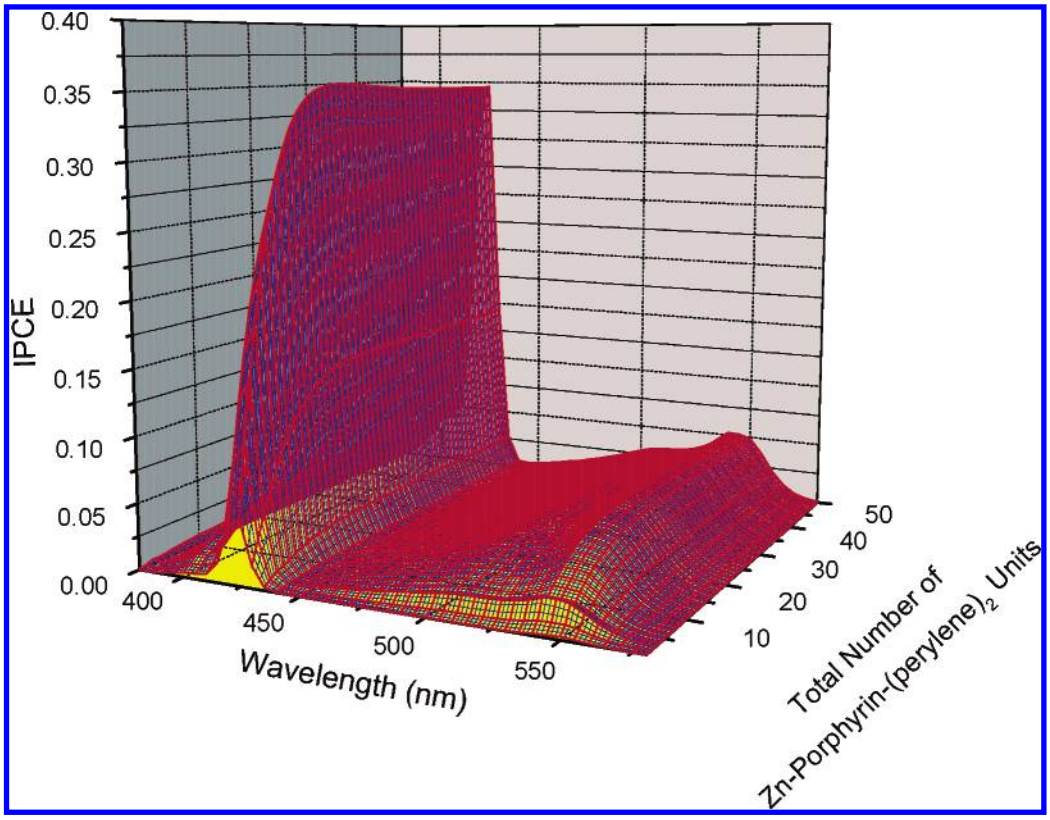

Figure 7. The calculated IPCE from 400 to 600 nm for porphyrin arrays with a 115 Å^2 footprint and the indicated number of Zn-porphyrin−(perylene)$_2$ units. Note that the unit closest to the array (unit 1) does not have perylenes attached to the zinc porphyrin, as indicated in Figure 2.

TABLE 4: Calculated Global Efficiencies (η) of Porphyrin Array-Containing Solar Cells as a Function of Array Length from the Kinetic Modeling (first row) and from the Upper-Limit Prediction that Each Absorbed Photon Yields an Electron in the Semiconductor (second row)[a]

porphyrin pigments (n)	1 η (%)	5 η (%)	10 η (%)	20 η (%)	50 η (%)
i_{sc} from calculations	0.12	0.17	0.19	0.33	0.23
i_{sc} from APCE = 1	0.12	0.57	1.08	1.98	4.06

[a] Calculations assumed AM 1.5 solar illumination, V_{oc} = 1.4 V, ff = 1, and footprint = 115 Å^2.

absorption coefficient is much lower than the porphyrin Soret band absorption coefficient (effective $\epsilon \approx 32\,000$ (two perylenes) vs 200 000 M^{-1} cm^{-1}), the optimum length of arrays is different with respect to absorption by perylenes versus porphyrins. This point is illustrated in Figure 7, which shows how the IPCE at each wavelength increases with array length. For a footprint of 115 Å^2, the optimal length with respect to the photocurrent derived from Soret band excitation is 30 porphyrin units. The lower molar absorption coefficient of the perylene units compared to the porphyrins results in a much more shallow increase in efficiency, with an optimal length of ∼50 porphyrin−(perylene)$_2$ units for absorption at 540 nm.

Global efficiencies (η) of porphyrin−(perylene)$_2$ arrays with 115 Å^2 footprints were computed (eq 4) with the integrated photocurrents calculated from the kinetic modeling. These efficiencies were compared with the theoretical maximum efficiencies that were calculated by assuming an APCE of unity; the results are shown in Table 4. In both cases, these efficiencies were calculated with nearly optimal V_{oc} values and fill factors equal to 1. For an array with only one pigment, the global efficiencies calculated by the two approaches were the same. This is because radiative and nonradiative decay could not compete with electron injection into the semiconductor. However, as the array became longer, the calculated global efficiencies became significantly lower than the optimal values, primarily due to competitive nonradiative decay processes. We emphasize that it is trivial to calculate the global AM 1.5 efficiency with the use of other input values (eq 4). However, it is not straightforward to predict a reasonable fill factor or V_{oc} value for an array-containing solar cell, as none has been constructed. As an estimate, one could assume the optimal values achieved for a Gratzel-type solar cell (V_{oc} = 0.8 and ff = 0.7).[40] Using these values would reduce the global efficiencies listed in Tables 3 and 4 by a factor of ∼2.5.

New Arrays for Higher Efficiency. The prediction of global efficiencies by the kinetic modeling approach outlined above is useful for designing new arrays. For example, consider a heteroporphyrin array consisting of 10 Zn(II)porphyrin−(perylene)$_2$ units (termed "ZnP"), 9 Mg(II)porphyrin−(perylene)$_2$ units (termed "MgP"), and a single terminal Mg(II)porphyrin unit (also termed "MgP") for surface attachment. The calculated electron-injection yield as a function of the number of pigments is shown in Figure 8. The calculation assumes an energy-transfer rate for MgP*−MgP → MgP−MgP* of (14 ps)$^{-1}$. The known energy-transfer rates for ZnP*−ZnP → ZnP− ZnP* and ZnP*−MgP → ZnP−MgP* are (30 ps)$^{-1}$ and (9 ps)$^{-1}$, respectively.[41,42] The energy-transfer process of MgP*−ZnP → MgP−ZnP* is energetically unfavored and does not occur. Thus, the ZnP−MgP connection functions effectively as a diode, funneling excited-state energy toward the semiconductor and preventing energy backflow.

The calculation predicts that the ZnP$_{10}$−MgP$_{10}$ system will perform more efficiently than the corresponding all-ZnP array. Absorption by the 10th or 20th unit will lead to injection with probability of 0.908 or 0.562, respectively. The corresponding

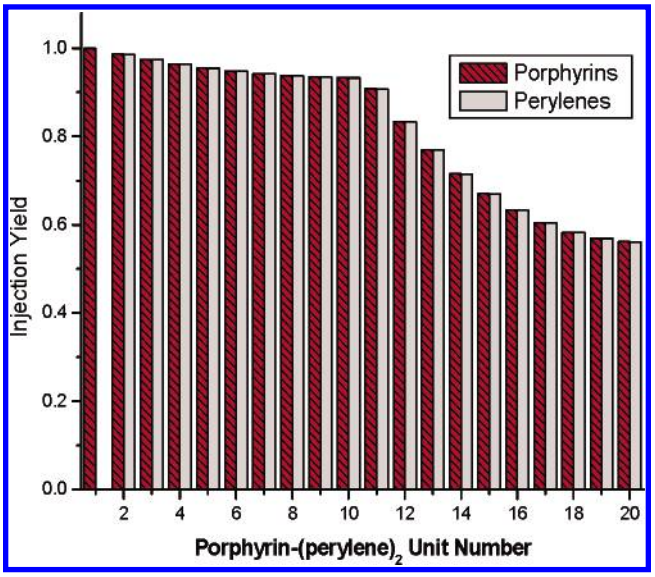

Figure 8. Injection probability for each pigment in the hypothetical $TiO_2-Mg(II)porphyrin_1-[Mg(II)porphyrin-(perylene)_2]_9-[Zn(II)porphyrin-(perylene)_2]_{10}$ array.

values for the all-Zn icosamer are 0.400 or 0.223. With a 115 Å^2 footprint, the predicted Soret band IPCE is 0.69 for the $ZnP_{10}-MgP_{10}$ array versus 0.63 for the ZnP_{20} array. Thus, the knowledge of energy-transfer rates for porphyrins, perylenes, phthalocyanines, chlorins, and bacteriochlorins will enable the design of arrays with "fine-tuned" energetics and optimized solar conversion efficiencies.

Conclusions

Theoretical predictions of the solar light-harvesting and energy-conversion properties have been made for linear arrays of weakly coupled porphyrinic pigments oriented on a semiconductor surface. The fraction of incident solar photons that are harvested increases with the number of pigments in the array, whereas the solar conversion efficiency is optimal with an intermediate number of pigments. The occurrence of an optimum intermediate length stems from the facts that (1) excited states formed far from the electrode surface cannot be efficiently collected because of competitive radiative and nonradiative relaxation pathways, and (2) excited-state energy will transfer in both directions along the light-harvesting array. The results underscore the need to carefully consider the detailed interfacial orientation, molar absorption coefficients, relaxation rates, and energy-transfer dynamics when designing light-harvesting arrays for solar cell applications. The approach described herein provides a formal mechanism for assessing the optimal number of pigments (i.e., the multilayer thickness) for solar conversion given the knowledge of fundamental parameters including pigment molar absorption coefficients, array packing density, excited-state lifetimes, and rates of interpigment energy-transfer processes. The pigments may be molecular dyes such as the porphyrins described herein or other discrete organic or inorganic chromophores. This fine-grained, bottom-up approach toward modeling photochemical features of synthetic materials of known architectures should facilitate the rational design of molecular-based solar cells.

Acknowledgment. This research was supported by grants from the Division of Chemical Sciences, Office of Basic Energy Sciences, Office of Energy Research, U. S. Department of Energy (D.F.B. (DE-FG02-05ER15660), D.H. (DE-FG02-05ER15661), J.L. (DE-FG02-96ER14632), and G.J.M. (DE-FG02-96ER14662)).

Appendix I: Kinetic Modeling of Energy Transfer Efficiencies in Porphyrin Arrays

The modeling of energy-transfer and electron-transfer processes is based on the approach of van Patten et al.[35] The proposed icosamer consists of 20 zinc porphyrins (**a** through **t**) and 38 perylene groups (**ap** through **sp**). The calculations predict the quantum efficiency that an absorbed photon yields an electron injected into the conduction band of TiO_2. Knowledge of the rate of every possible energy-transfer or electron-transfer event (there is a total of $59 \times 58 = 3422$) would enable calculation of the efficiency of energy migration through the system. Presumably, many of these rates will be small by comparison to those involving nearest-neighbor units, e.g., **ap** going directly to **t** versus **ap** → **a** → **b** → ... → **t**. Thus, we ignore long-range and through-space energy-transfer events and consider only energy transfer between adjacent pigments. We note that recent work has shown that energy-transfer processes between first non-nearest-neighbor porphyrins have rate constants that are, on the average, an order of magnitude lower than for nearest neighbors.[41,43,44] Depending on the symmetry of the array and the number of sites involved, the presence of such non-nearest-neighbor processes may result in a shortening of the rate and an increase in the yield of overall energy transfer to the pigment adjacent to the trap site (surface).[41] However, these processes are not included here because of the large number of additional parameters that would be incorporated into the model, and their absence will not affect the qualitative conclusions of the study. Furthermore, we assume that the experimentally determined rates in model systems do not change significantly upon incorporation of the chromophore building blocks into large arrays or upon adsorption of arrays to the semiconductor surface. Two perylene groups attached to one porphyrin are treated as one unit with a molar absorption coefficient that is twice as large. A total of 39 excited-state species and the charge-separated state $ZnP_{19}-ZnP^+-TiO_2|(e^-)$, where an electron is injected into the semiconductor, will be considered.

The following energy-transfer or electron-transfer processes are taken into account:

$$k_1:\ ZnP^*-ZnP \rightarrow ZnP-ZnP^*, \quad \text{energy transfer towards the surface} \tag{A1}$$

$$k_{-1}:\ ZnP-ZnP^* \rightarrow ZnP^*-ZnP, \quad \text{energy transfer away from the surface} \tag{A2}$$

$$k_2:\ \text{perylene}^* + ZnP \rightarrow \text{perylene} + ZnP^* \tag{A3}$$

$$k_3:\ ZnP^* \rightarrow ZnP + h\nu, \text{ or } \Delta \tag{A4}$$

$$k_4:\ \text{perylene}^* \rightarrow \text{perylene} + h\nu \text{ or } \Delta \tag{A5}$$

(k_3 and k_4 include radiative and nonradiative decay; in particular, these rate constants are the inverse of the excited-state lifetime of the corresponding monomeric chromophore in the absence of energy transfer or electron transfer)

$$k_{inj}:\ ZnP^* + TiO_2 \rightarrow ZnP^+ + TiO_2|(e^-), \quad \text{electron transfer into the semiconductor} \tag{A6}$$

The rate constants have the following values: $k_1 = k_{-1} = (30\ \text{ps})^{-1}$, $k_2 = (3.5\ \text{ps})^{-1}$, $k_3 = (2.4\ \text{ns})^{-1}$, $k_4 = (30\ \text{ns})^{-1}$, and $k_{inj} = (300\ \text{fs})^{-1}$, respectively.[23,35,41]

The rates of change are given by the following equations:

$$\frac{dA}{dt} = k_2[\mathbf{ap}] + k_{-1}[\mathbf{b}] - (k_1 + k_3)[\mathbf{a}] \quad \text{(A7)}$$

$$\frac{dB}{dt} = k_2[\mathbf{bp}] + k_1[\mathbf{a}] + k_{-1}[\mathbf{c}] - (k_1 + k_3)[\mathbf{b}] \quad \text{(A8)}$$

$$\vdots$$

$$\frac{dT}{dt} = k_1[\mathbf{s}] - (k_{-1} - k_{inj} - k_3)[T] \quad \text{(A9)}$$

$$\vdots$$

$$\frac{d[\mathbf{sp}]}{dt} = -(k_2 + k_4)[\mathbf{sp}] \quad \text{(A10)}$$

$$\frac{d[TiO_2 \mid (e^-)]}{dt} = k_{inj}[T] \quad \text{(A11)}$$

This set of coupled differential equations can be written in matrix form

$$\mathbf{W}\cdot\mathbf{z} = \frac{d}{dt}\mathbf{z} \quad \text{(A12)}$$

Where

$$\mathbf{z} = \begin{pmatrix} [A] \\ [B] \\ \vdots \\ [TiO_2] \end{pmatrix} \text{ and } \mathbf{W} = \begin{pmatrix} -k_1 - k_3 & k_{-1} & \cdots & 0 \\ k_1 & -k_1 - k_{-1} - k_3 & \cdots & 0 \\ \vdots & \vdots & \ddots & \vdots \\ 0 & 0 & \cdots & k_{inj} \end{pmatrix}$$

The next step is the determination of eigenvectors and eigenvalues of $\mathbf{W}$.

$$\mathbf{X}_L\cdot\mathbf{W}\cdot\mathbf{X}_R = \lambda \quad \text{(A13)}$$

Since $\mathbf{X}_L$ and $\mathbf{X}_R$ are inverses, we can write eq A12 as

$$\mathbf{W}\cdot\mathbf{X}_R\cdot\mathbf{X}_L\cdot\mathbf{z} = \frac{d}{dt}\mathbf{z} \quad \text{(A14)}$$

Left multiplying eq A14 with $\mathbf{X}_L$, and using eq A13, gives

$$\lambda\cdot(\mathbf{X}_L\cdot\mathbf{z}) = \frac{d}{dt}(\mathbf{X}_L\cdot\mathbf{z}) \quad \text{(A15)}$$

We define $\mathbf{U}(t) = \mathbf{X}_L\cdot\mathbf{z}$. Equation A15 can easily be integrated

$$\lambda_i\cdot\mathbf{U}_i(t) = \frac{d}{dt}\mathbf{U}_i \rightarrow \mathbf{U}_i(t) = U_{io}\exp[\lambda_i\cdot t] \quad \text{(A16)}$$

The values for U_{io} are determined by imposing initial conditions on the equation

$$\mathbf{z} = \mathbf{X}_R\cdot\mathbf{U}(t) \quad \text{(A17)}$$

for example, $t = 0$; $z_1 = 1$; $z_{i\neq 1} = 0$ corresponds to the case where only the porphyrin furthest from the surface is in the excited-state initially. The final value of the concentration of $TiO_2|(e^-)$ is simply the probability that electron injection occurs if porphyrin A absorbs a photon. In this manner, the plots showing the probability of injection (Figures 3 and 6) are generated. Likewise, $z_i = [(1 - \alpha_1)^{20-i}\cdot\alpha_1]$, for $i = 1-20$ gives the initial values (Figure 2b), taking into account that porphyrins closer to the surface absorb more light than those further away under operating conditions of a solar cell.

References and Notes

(1) (a) Ross, R. T.; Calvin, M. *Biophys. J.* **1967**, *7*, 595−614. (b) Knox, R. S. *Biophys. J.* **1969**, *9*, 1351−1362. (c) Bjorn, I. O. *Photosynthetica* **1976**, *10*, 121−129.

(2) Shockley, W.; Queisser, H. J. *J. Appl. Phys.* **1961**, *32*, 510−514.

(3) Ross, R. T.; Nozik, A. J. *J. Appl. Phys.* **1982**, *53*, 3813−3818.

(4) Ambroise, A.; Kirmaier, C.; Wagner, R. W.; Loewe, R. S.; Bocian, D. F.; Holten, D.; Lindsey, J. S. *J. Org. Chem.* **2002**, *67*, 3811−3826.

(5) Loewe, R. S.; Tomizaki, K.-Y.; Youngblood, W. J.; Bo, Z.; Lindsey, J. S. *J. Mater. Chem.* **2002**, *12*, 3438−3451.

(6) del Rosario Benites, M.; Johnson, T. E.; Weghorn, S.; Yu, L.; Rao, P. D.; Diers, J. R.; Yang, S. I.; Kirmaier, C.; Bocian, D. F.; Holten, D.; Lindsey, J. S. *J. Mater. Chem.* **2002**, *12*, 65−80.

(7) Holten, D.; Bocian, D. F.; Lindsey, J. S. *Acc. Chem. Res.* **2002**, *35*, 57−69.

(8) Seth, J.; Palaniappan, V.; Johnson, T. E.; Prathapan, S.; Lindsey, J. S.; Bocian, D. F. *J. Am. Chem. Soc.* **1994**, *116*, 10578−10592.

(9) Seth, J.; Palaniappan, V.; Wagner, R. W.; Johnson, T. E.; Lindsey, J. S.; Bocian, D. F. *J. Am. Chem. Soc.* **1996**, *118*, 11194−11207.

(10) Loewe, R. S.; Lammi, R. K.; Diers, J. R.; Kirmaier, C.; Bocian, D. F.; Holten, D.; Lindsey, J. S. *J. Mater. Chem.* **2002**, *12*, 1530−1552.

(11) O'Neil, M. P.; Niemczyk, M. P.; Svec, W. A.; Gosztola, D.; Gaines, G. L.; Wasielewski, M. R. *Science* **1992**, *257*, 63−65.

(12) van der Boom, T.; Hayes, R. T.; Zhao, Y. Y.; Bushard, P. J.; Weiss, E. A.; Wasielewski, M. R. *J. Am. Chem. Soc.* **2002**, *124*, 9582−9590.

(13) Ahrens, M. J.; Sinks, L. E.; Rybtchinski, B.; Liu, W. H.; Jones, B. A.; Giaimo, J. M.; Gusev, A. V.; Goshe, A. J.; Tiede, D. M.; Wasielewski, M. R. *J. Am. Chem. Soc.* **2004**, *126*, 8284−8294.

(14) Hayes, R. T.; Walsh, C. J.; Wasielewski, M. R. *J. Phys. Chem. A* **2004**, *108*, 3253−3260.

(15) Kelley, R. F.; Tauber, M. J.; Wasielewski, M. R. *J. Am. Chem. Soc.* **2006**, *128*, 4779−4791.

(16) Wasielewski, M. R. *J. Org. Chem.* **2006**, *71*, 5051−5066.

(17) You, C. C.; Wurthner, F. *Org. Lett.* **2004**, *6*, 2401−2404.

(18) Miller, M. A.; Lammi, R. K.; Prathapan, S.; Holten, D.; Lindsey, J. S. *J. Org. Chem.* **2000**, *65*, 6634−6649.

(19) Prathapan, S.; Yang, S. I.; Seth, J.; Miller, M. A.; Bocian, D. F.; Holten, D.; Lindsey, J. S. *J. Phys. Chem. B* **2001**, *105*, 8237−8248.

(20) Yang, S. I.; Prathapan, S.; Miller, M. A.; Seth, J.; Bocian, D. F.; Lindsey, J. S.; Holten, D. *J. Phys. Chem. B* **2001**, *105*, 8249−8258.

(21) Yang, S. I.; Lammi, R. K.; Prathapan, S.; Miller, M. A.; Seth, J.; Diers, J. R.; Bocian, D. F.; Lindsey, J. S.; Holten, D. *J. Mater. Chem.* **2001**, *11*, 2420−2430.

(22) Kirmaier, C.; Yang, S. I.; Prathapan, S.; Miller, M. A.; Diers, J. R.; Bocian, D. F.; Lindsey, J. S.; Holten, D. *Res. Chem. Intermed.* **2002**, *28*, 719−740.

(23) Tomizaki, K.; Loewe, R. S.; Kirmaier, C.; Schwartz, J. K.; Retsek, J. L.; Bocian, D. F.; Holten, D.; Lindsey, J. S. *J. Org. Chem.* **2002**, *67*, 6519−6534.

(24) Loewe, R. S.; Tomizaki, K.-Y.; Chevalier, F.; Lindsey, J. S. *J. Porphyrins Phthalocyanines* **2002**, *6*, 626−642.

(25) (a) Muthukumaran, K.; Loewe, R. S.; Kirmaier, C.; Hinden, E.; Schwartz, J. K.; Sazanovich, I. V.; Diers, J. R.; Bocian, D. F.; Holten, D.; Lindsey, J. S. *J. Phys. Chem. B* **2003**, *107*, 3431−3442. (b) Kirmaier, C.; Hinden, E.; Schwartz, J. K.; Sazanovich, I. V.; Diers, J. R.; Muthukumaran, K.; Taniguchi, M.; Bocian, D. F.; Lindsey, J. S.; Holten, D. *J. Phys. Chem. B* **2003**, *107*, 3443−3454.

(26) Tomizaki, K.-Y.; Thamyongkit, P.; Loewe, R. S.; Lindsey, J. S. *Tetrahedron* **2003**, *59*, 1191−1207.

(27) (a) Smestad, G.; Bignozzi, C. A.; Argazzi, R. *Sol. Energy Mater. Sol. Cells* **1994**, *32*, 259−272. (b) Smestad, G. *Sol. Energy Mater. Sol. Cells* **1994**, *32*, 273−288.

(28) Gerischer, H. *Photochem. Photobiol.* **1972**, *16*, 243−260.

(29) Clark, W. D. K.; Sutin, N. *J. Am. Chem. Soc.* **1977**, *99*, 4676−4682.

(30) Sonntag, L. P.; Spitler, M. T. *J. Phys. Chem.* **1985**, *89*, 1453−1457.

(31) Schick, A. G.; Schreiman, I. C.; Wagner, R. W.; Lindsey, J. S.; Bocian, D. F. *J. Am. Chem. Soc.* **1989**, *111*, 1344−1350.

(32) Lakowicz, J. R. *Principles of Fluorescence Spectroscopy*, 2nd ed.; Plenum Publishers: New York, 1999.

(33) Dixon, J. M.; Taniguchi, M.; Lindsey, J. S. *Photochem. Photobiol.* **2005**, *81*, 212−213.

(34) Vanden Berghe, R. A. L.; Cardon, F.; Gomes, W. P. *Surf. Sci.* **1973**, *39*, 368−384.

(35) Van Patten, P. G.; Shreve, A. P.; Lindsey, J. S.; Donohoe, R. J. *J. Phys. Chem. B* **1998**, *102*, 4209−4216.
(36) Whalley, M. *J. Chem. Soc.* **1961**, 866−869.
(37) Ficken, G. E.; Linstead, R. P. *J. Chem. Soc.* **1952**, 4846−4854.
(38) Taniguchi, M.; Kim, H.-J.; Ra, D.; Schwartz, J. K.; Kirmaier, C.; Hindin, E.; Diers, J. R.; Prathapan, S.; Bocian, D. F.; Holten, D.; Lindsey, J. S. *J. Org. Chem.* **2002**, *67*, 7329−7342.
(39) Hoebeke, M.; Damoiseau, X.; Schuitmaker, H. J.; Van de Vorst, A. *Biochim. Biophys. Acta* **1999**, *1420*, 73−85.
(40) Gratzel, M. *Inorg. Chem.* **2005**, *44*, 6841−6851.
(41) Hindin, E.; Forties, R. A.; Loewe, R. S.; Ambroise, A.; Kirmaier, C.; Bocian, D. F.; Lindsey, J. S.; Holten, D.; Knox, R. S. *J. Phys. Chem. B* **2004**, *108*, 12821−12832.
(42) Hascoat, P.; Yang, S. I.; Lammi, R. K.; Alley, J.; Bocian, D. F.; Lindsey, J. S.; Holten, D. *Inorg. Chem.* **1999**, *38*, 4849−4853.
(43) Lammi, R. K.; Ambroise, A.; Balasubramanian, T.; Wagner, R. W.; Bocian, D. F.; Holten, D.; Lindsey, J. S. *J. Am. Chem. Soc.* **2000**, *122*, 7579−7591.
(44) Lammi, R. K.; Ambroise, A.; Wagner, R. W.; Diers, J. R.; Bocian, D. F.; Holten, D.; Lindsey, J. S. *Chem. Phys. Lett.* **2001**, *341*, 35−44.